

Multiwavelength spectral evolution during the 2011 outburst of the very faint X-ray transient Swift J1357.2–0933

M. Armas Padilla¹*, N. Degenaar², D. M. Russell³ and R. Wijnands¹

¹Astronomical Institute "Anton Pannekoek", University of Amsterdam, Postbus 94249, 1090 GE Amsterdam, The Netherlands

²University of Michigan, Department of Astronomy, 500 Church St, Ann Arbor, MI 48109, USA

³Instituto de Astrofísica de Canarias (IAC), Vía Láctea s/n, La Laguna 38205, S/C de Tenerife, Spain

26 July 2012

ABSTRACT

We report our multiwavelength study of the 2011 outburst evolution of the newly discovered black hole candidate X-ray binary Swift J1357.2–0933. We analysed the *Swift* X-ray telescope and Ultraviolet/Optical telescope (UVOT) data taken during the ~ 7 months duration of the outburst. It displayed a 2–10 keV X-ray peak luminosity of $\sim 10^{35} (\text{D}/1.5 \text{ kpc})^2 \text{ erg s}^{-1}$ which classifies the source as a very faint X-ray transient. We found that the X-ray spectrum at the peak was consistent with the source being in the hard state, but it softened with decreasing luminosity, a common behaviour of black holes at low luminosities or returning to quiescence from the hard state. The correlations between the simultaneous X-ray and ultraviolet/optical data suggest a system with a black hole accreting from a viscous disc that is not irradiated. The UVOT filters provide the opportunity to study these correlations up to ultraviolet wavelengths a regime so far unexplored. If the black hole nature is confirmed, Swift J1357.2–0933 would be one of the very few established black hole very-faint X-ray transients.

Key words: X-rays:binaries – stars:individual: Swift J1357.2–0933 – accretion, accretion discs

1 INTRODUCTION

X-ray binaries are the brightest X-ray point sources in our Galaxy. They are black holes (BH) or neutron stars (NS) accreting material from a companion star. The transient X-ray binaries alternate long epochs of quiescence during which they have X-ray luminosities of $L_X \sim 10^{30-33} \text{ erg s}^{-1}$ with outburst episodes during which the luminosity increases more than two orders of magnitude. The systems that reach a peak X-ray luminosity of only $L_X^{\text{peak}} \sim 10^{34-36}$ are called *very-faint* X-ray binary transients (VFXTs). They are at their peaks 2–5 orders of magnitude fainter than the better studied *faint* and *bright* systems ($L_X^{\text{peak}} \sim 10^{36-39} \text{ erg s}^{-1}$; Wijnands et al. 2006).

It is in the last decade that VFXTs have been investigated in detail thanks to the improvement in sensitivity and resolution of the X-ray instruments in orbit. However, even though the number of known sources has increased, their characteristics are still not well known. A considerable fraction of them have exhibited thermonuclear X-ray Type-I bursts, identifying the accretor as a NS (eg. Cornelisse et al. 2002; Del Santo et al. 2007; Chelovekov & Grebenev 2007; Degenaar & Wijnands 2009).

Swift J1357.2–0933 is a new VFXT discovered with the Swift Burst Alert Telescope (BAT) on 2011 January 28 (Krimm et al.

2011). In the following days it was observed with several X-ray satellites as well as ground-based telescopes. The MPI/ESO 2.2m telescope at La Silla detected a new optical source within the *Swift*/BAT error circle. The magnitude difference compared to archival Sloan Digital Sky Survey (SDSS) images (when the source was in quiescence) was ~ 6 mag. This indicates a Galactic origin, likely a low mass X-ray binary (LMXB) or a dwarf nova outburst (Rau et al. 2011), although the X-ray spectrum pointed to a LMXB nature (Krimm et al. 2011). The SDSS photometry indicated that the quiescent counterpart was very red and that the companion was likely an M4 star. This resulted in a distance estimate of ~ 1.5 kpc (Rau et al. 2011). In this work we present analysis of the *Swift* X-ray and ultraviolet–optical (UV/optical) data of Swift J1357.2–0933 along its 2011 outburst.

2 OBSERVATIONS AND ANALYSIS

Immediately following its discovery Swift J1357.2–0933 was monitored with the *Swift* X-ray telescope (XRT) and the Ultraviolet/Optical telescope (UVOT) throughout its outburst, which lasted ~ 7 months. A total of 42 pointings were performed during this period, for a total exposure time of 54.8 ks. A log of the observations is given in Table 1. The observations were performed daily in the first 10 days, and once every 2 days in the following month. After that, the observations were separated by 1 to 2 weeks.

* E-mail: M.Armaspadilla@uva.nl

Table 1. Log and XRT spectral results for Swift J1357.2–0933.

Obs-ID	Date	Mode	Exp-time (ksec)	Γ	$F_{X,abs}^a$	$F_{X,unabs}^a$	L_X^b	$\chi^2_{\nu}/\text{d.o.f.}$
31918002	2/1/11	WT	3.28	1.53 ± 0.02	415 ± 6	419 ± 6	113 ± 2	0.98 / 323
31918003	2/2/11	WT	0.98	1.59 ± 0.03	382 ± 7	386 ± 7	104 ± 2	1.07 / 258
31918004	2/3/11	WT	1.63	1.56 ± 0.03	404 ± 7	408 ± 7	110 ± 2	0.95 / 263
31918005	2/4/11	WT	1.65	1.56 ± 0.02	373 ± 6	378 ± 6	102 ± 1	0.98 / 313
31918007	2/6/11	WT	1	1.54 ± 0.03	368 ± 7	372 ± 7	100 ± 2	0.96 / 250
31918008	2/7/11	WT	1.1	1.54 ± 0.03	348 ± 7	352 ± 7	94.8 ± 1.8	0.97 / 260
31918009	2/8/11	WT	1.74	1.52 ± 0.03	345 ± 6	349 ± 6	94.0 ± 1.6	1.10 / 274
31918010	2/9/11	WT	1.14	1.57 ± 0.03	329 ± 6	333 ± 6	89.5 ± 1.7	0.88 / 244
31918011	2/10/11	WT	1.03	1.55 ± 0.03	317 ± 7	321 ± 6	86.4 ± 1.7	1.11 / 240
31918012	2/11/11	WT	1.19	1.57 ± 0.03	309 ± 6	313 ± 6	84.2 ± 1.5	0.93 / 260
31918013	2/16/11	WT	1	1.53 ± 0.03	299 ± 6	302 ± 6	81.3 ± 1.7	0.99 / 224
31918014	2/18/11	WT	1.25	1.55 ± 0.03	263 ± 5	266 ± 5	71.7 ± 1.4	0.90 / 239
31918015	2/20/11	WT	1.08	1.53 ± 0.04	233 ± 6	236 ± 5	63.4 ± 1.5	0.89 / 189
31918016	2/24/11	WT	0.49	1.57 ± 0.05	207 ± 7	209 ± 7	56.3 ± 2.0	1.04 / 99
31918017	2/26/11	WT	1.11	1.62 ± 0.04	176 ± 4	179 ± 4	48.1 ± 1.1	0.92 / 173
31918018	2/28/11	WT	1.39	1.58 ± 0.04	171 ± 4	174 ± 4	46.7 ± 1.1	0.77 / 203
31918019	3/2/11	WT	1.35	1.57 ± 0.04	161 ± 4	163 ± 4	43.9 ± 1.0	0.90 / 185
31918020	3/4/11	WT	1.31	1.54 ± 0.04	150 ± 4	152 ± 4	40.8 ± 1.0	1.01 / 174
31918021	3/6/11	WT	1.31	1.59 ± 0.04	133 ± 4	135 ± 4	36.3 ± 1.0	0.88 / 141
31918022	3/8/11	WT	1.3	1.53 ± 0.04	147 ± 4	149 ± 4	40.0 ± 1.0	0.95 / 160
31918023	3/10/11	WT	1.2	1.56 ± 0.04	126 ± 4	128 ± 4	34.4 ± 1.0	0.79 / 131
31918024	3/12/11	WT	1.38	1.58 ± 0.05	134 ± 4	135 ± 4	36.4 ± 1.1	1.10 / 114
31918025	3/13/11	WT	1.23	1.59 ± 0.05	108 ± 3	110 ± 3	29.5 ± 0.9	1.17 / 122
31918026	3/16/11	WT	0.25	1.54 ± 0.12	82.0 ± 6.8	82.9 ± 6.8	22.3 ± 1.8	1.04 / 22
31918027	3/18/11	WT	1.21	1.6 ± 0.05	88.13 ± 2.9	89.2 ± 2.9	24.0 ± 0.8	0.94 / 102
31918028	3/20/11	WT	1.22	1.56 ± 0.09	102 ± 6	103 ± 6	27.7 ± 1.6	0.91 / 45
31918029	3/29/11	WT	1.27	1.6 ± 0.06	79.6 ± 3.2	80.6 ± 3.2	21.7 ± 0.9	0.97 / 76
31918030	4/3/11	WT	1.45	1.63 ± 0.06	65.4 ± 2.3	66.3 ± 2.3	17.8 ± 0.6	0.91 / 93
31918031	4/13/11	WT	1.34	1.54 ± 0.11	47.7 ± 3.4	48.2 ± 3.3	13.0 ± 0.9	0.53 / 29
31918032	4/20/11	WT	1.56	1.69 ± 0.07	37.8 ± 1.7	38.3 ± 1.7	10.3 ± 0.4	0.97 / 60
31918033	4/23/11	WT	1.26	1.63 ± 0.08	36.5 ± 1.9	36.9 ± 1.9	9.95 ± 0.51	0.83 / 49
31918034	4/28/11	WT	1.24	1.82 ± 0.14	20.6 ± 1.7	20.9 ± 1.7	5.63 ± 0.45	1.30 / 26
31918035	5/3/11	WT	1.12	1.83 ± 0.1	29.3 ± 1.7	29.8 ± 1.7	8.02 ± 0.45	0.95 / 38
31918036	5/8/11	WT	1.02	1.75 ± 0.12	22.7 ± 1.7	23.1 ± 1.7	6.21 ± 0.45	1.01 / 25
31918037	5/13/11	WT	1.34	1.75 ± 0.12	22.6 ± 1.7	23.0 ± 1.7	6.18 ± 0.46	1.21 / 21
31918038	6/15/11	PC	1.15	1.94 ± 0.24	5.42 ± 0.67	5.52 ± 0.66	1.49 ± 0.18	1.03 / 31
31918039	6/29/11	PC	1.24	1.93 ± 0.26	3.90 ± 0.54	3.97 ± 0.53	1.07 ± 0.14	0.98 / 23
31918040	7/14/11	PC	1.07	1.8 ± 0.45	3.22 ± 0.83	3.27 ± 0.81	0.88 ± 0.22	0.96 / 10
31918041	7/28/11	PC	0.65	$2.19^{+1.91}_{-0.98}$	1.64 ± 0.85	1.68 ± 0.92	0.45 ± 0.24	1.21 / 4
31918043	8/23/11	PC	1.19	2.19 (fix)	< 0.26	< 0.27	< 0.07	–
31918044	9/5/11	PC	2.05	2.19 (fix)	< 0.09	< 0.09	< 0.02	–

Note.- N_H has been fixed to $1.2 \times 10^{20} \text{ cm}^{-2}$, the value obtained from Krimm et al. (2011).

^a Flux in units of $10^{-12} \text{ erg cm}^{-2} \text{ s}^{-1}$ in the 0.5–10 keV energy band.

^b X-ray luminosity in units of $10^{33} \text{ erg s}^{-1}$ calculated from the 0.5–10 keV unabsorbed flux by adopting a distance of 1.5 kpc.

2.1 XRT data

The *Swift*/XRT observations were obtained both in photon-counting (PC) and windowed timing (WT) modes. Due to the high flux of Swift J1357.2–0933 the XRT was operated in the WT mode in the early observations in order to avoid pile-up (except for the first observation; see below). When the count rate was below 0.5 count/s the observations were taken in the PC mode (see Table 1). The data were processed running the `xrtpipeline` task in which standard event grades of 0–12 were selected for the PC data and 0–2 for the WT mode observations.

For every observation, spectra, lightcurves and images were obtained using `Xselect` (v.2.4b). For the WT data, we used a circle of ~ 27 pixels of radius to extract the source events and

for the background extraction we used an annulus centred on the source with ~ 64 pixels for the inner radius and ~ 91 pixels (64+27) for the outer radius. In the case of the PC mode observations, the region used was a circle of ~ 10 pixels of radius for the source and for the background three circular regions with the same size located in nearby source-free regions.

To look for eclipses, dips or X-ray bursts we checked the lightcurves with different bin-sizes extracted for each observation. We did not detect any evidence of feature that suggest modulations or a patron in the source flux, although the statistic of our data is not very good. We created the exposure maps in order to correct for the effect of bad columns on the CCD, which in turn are used to create the ancillary response files using the `xrtmkarf` task.

The latest versions of the response matrix files (v.11) were taken from the HEASARC calibration database. Finally, with `grppha` we grouped the spectra to have a minimum of 20 photons per bin, except for the observations 38/39/40/41¹, where 5 photons per bin was used due to the low number of counts collected during those observations.

The first observation 01 was taken in PC mode, which provided the source position with an error of 2.1 arcsec (Krimm et al. 2011). However, it is severely affected by pile-up. It has a count rate of 2.3 c/s, while the pile-up becomes considerable in PC mode for count rates above ~ 0.5 c/s. Therefore we do not include this observation in our analysis. In the last two XRT observations (43/44) the source was not detected. The count rates were calculated using the prescription for small numbers of counts given by Gehrels (1986). We calculated the 95 per cent confidence upper limits on the flux with WebPIMMS HEARSAC tool². An absorbed power-law model with a hydrogen column density (N_H) of $1.2 \times 10^{20} \text{ cm}^{-2}$ (see Section 3) was assumed. We used a photon index of $\Gamma=2.19$ which corresponds to the value we obtained in the last observation where the source was detected.

In order to improve the statistics we have also combined observations that were performed within a few days time span and that yielded comparable fluxes. As such, we have combined observations 03–05, 07–12, 13–15, 17–20, 21–25, 26–20, 30–33, 34–37, 38–41 and 43–44. We extracted the combined spectra, lightcurves and images with `Xselect` (v.2.4b) in the same way as the individual cases. We merged the individual exposure maps created for each image using the task `ximage`.

2.2 UVOT data

The UVOT observations were performed in image mode. Most of them were taken with 6 filters (*v*, *b*, *u*, *uvw1*, *uvm2*, *uvw2*) but some of them with only few filters and sometimes only one. The pre-processed images by the *Swift* Data Centre were already correctly aligned to the World Co-ordinate System. For each observation we summed the sky image for each filter to increase the photon statistic using the `uvotimsum` task. We calculated the source’s magnitude and flux densities with the `uvotsource` tool, which performs aperture photometry on the resulting summed sky images. We selected a circular region with a radius of 5 arcsec centred on the source and a circular region source-free with a radius of 18 arcsec for the background correction. We corrected the magnitudes and fluxes for the Galactic extinction. The reddening is $E(B-V)=0.04$ mag in the direction of Swift J1357.2–0933 (Schlegel et al. 1998). Using this value and the prescription of Pei (1992) we calculate the extinction for every band. The obtained values are $A_v=0.123$, $A_b=0.163$, $A_u=0.193$, $A_{uvw1}=0.263$, $A_{uvm2}=0.387$ and $A_{uvw2}=0.349$. The `uvotsource` tool returns also the magnitude upper limit in case of not source detection, in our case, a magnitude 3-sigma upper limit.

3 RESULTS

3.1 X-ray light curve and spectra

We fitted the spectra using `XSPEC` (v 12.7.0). All observations were well fitted with a simple power law affected by absorption. We assume a column density to Swift J1357.2–0933 of $1.2 \times 10^{20} \text{ cm}^{-2}$ and constant with time. We inferred this value from the high-resolution X-ray spectra obtained with *XMM-Newton* (Armas Padilla et al. 2012 in prep) and which in turns is consistent with the number reported by Krimm et al. (2011). We also tried several one and two component models (e.g. `bbbodyrad`, `diskbb`, `diskbb+powerlaw`) to fit the spectra, however the *Swift* data is of a too low statistical quality to distinguish between them. The results are reported in Table 1.

In Fig. 1 we show the 0.5–10 keV light curve. The outburst has its maximum as observed during observation 02 in the beginning³, where the peak of the unabsorbed flux is $4.2 \times 10^{-10} \text{ erg cm}^{-2} \text{ s}^{-1}$. It corresponds to a peak luminosity of $1.1 \times 10^{35} \text{ erg s}^{-1}$ assuming a distance of 1.5 kpc (Rau et al. 2011). After this, the luminosity monotonically decreases until the source went undetected using the XRT ~ 180 days after the discovery date. The upper-limits on the luminosity calculated from the last two observations are between 2 and $7 \times 10^{31} \text{ erg s}^{-1}$.

Plotting the photon index evolution with time (Fig. 1) it is clear that the photon index increases from a value of $\Gamma \sim 1.5$ to a value of $\Gamma \sim 2$ indicating that the spectra became softer during the decay of the outburst. This softening behaviour is also seen when using the hardness ratio (HR; Fig.1 left panel). The hardness ratio is defined as the ratio between the counts in the hard band (2–10 keV) and the counts in the soft band (0.5–2 keV). We have performed the same analysis on the combined data sets (see Section 2.1). The result is shown in Fig. 1 right panel. Due to the smaller error bars, the increase of the photon index and the HR decay are more clearly visible.

3.2 Ultraviolet/optical and X-ray correlation

The *Swift*/UVOT observations were taken simultaneously with the X-ray ones. Most of the observations were taken with all six filters, which allows us to study the correlation between the X-ray and the UV/optical emission along the outburst. Fig. 2 shows the X-ray and UV/optical light curves. The last UVOT detection (*u* band) was 203 days after the first detection when the source was already undetected in X-ray. Over the course of the outburst the brightness in all bands is decreasing similarly to the decline in the X-rays. This resulted in a clear correlation between X-ray and UV/optical fluxes which is shown in Fig. 3. We have assumed a power-law model to fit these correlations and calculate the correlation slopes β ($F_{UV/optical} \propto F_X^\beta$). We have calculated β for every UVOT band and for the X-ray flux in the 2–10 keV energy range in order to compare them with the values tabulated in previous publications (e.g. Russell et al. 2006). However, the spectral resolution of *Swift*/XRT allows us to get the correlations slopes also for X-ray fluxes in the 0.5–10 keV energy range. The results are shown in Table 2. Clearly β increases towards shorter wavelengths, going from 0.2 in the *v* band to 0.37 *uvw2* (using the 0.5–10 keV energy range).

¹ We refer to the observations with the last two numbers of their observation-ID’s in the main text. The full observation-ID’s are in Table 1

² Available from <http://heasarc.gsfc.nasa.gov/Tools/w3pimms.html>

³ Observation 01 could be brighter, but due to the strong pile-up it was not included in the analysis.

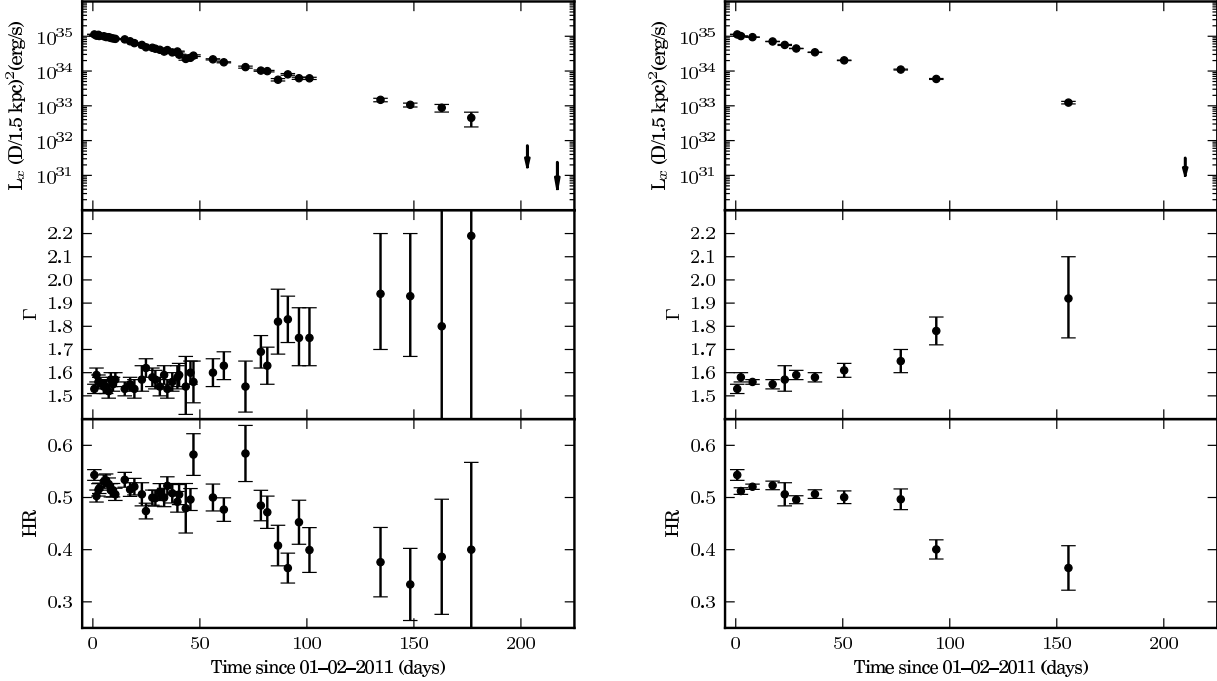


Figure 1. In both plots the upper panel is the light curve (0.5–10 keV; assumed distance of 1.5 kpc), the central panel is the photon index evolution with time, and the bottom panel is the hardness ratio evolution with the time (ratio of the counts in the hard, 2–10 keV, and soft, 0.5–2 keV energy bands). All data are plotted in the left figure, whereas the right figure presents the result of the combined observations.

Table 2. Correlation slope between UV/optical and X-ray fluxes ($F_{UV/optical} \propto F_X^\beta$). λ_{eff} is the effective wavelength for each band.

UVOT/Band	λ_{eff} (Å)	β	
		0.5–10 KeV	2–10 keV
v	5402	0.204 ± 0.019	0.198 ± 0.017
b	4329	0.239 ± 0.011	0.231 ± 0.011
u	3501	0.292 ± 0.007	0.283 ± 0.006
uvw1	2634	0.319 ± 0.007	0.305 ± 0.006
uvm2	2231	0.375 ± 0.007	0.355 ± 0.006
uvw2	2030	0.370 ± 0.006	0.356 ± 0.005

The numbers become 0.19 to 0.35 in the 2–10 keV range (see Fig. 4).

4 DISCUSSION

We have analysed the XRT and UVOT data taken over the ~ 7 months duration of the 2011 outburst of the newly discovered candidate black hole LMXB Swift J1357.2–0933. We fitted the *Swift*/XRT spectra using a simple power-law model affected by absorption. The peak flux was reached at the beginning of the outburst, after which, it steadily decreased until the source went undetected with XRT ~ 180 days after its discovery. The unabsorbed peak flux has a value of $F_{X,unabs} = 4.2 \times 10^{-10} \text{ erg cm}^{-2} \text{ s}^{-1}$ in the 0.5–10 keV energy range, which corresponds to an outburst peak luminosity of $L_X = 1.1 \times 10^{35} \text{ erg s}^{-1}$ assuming a distance of

1.5 kpc. This low peak luminosity classifies Swift J1357.2–0933 as a VFXT, which have a peak luminosities $L_X^{peak} < 10^{36} \text{ erg s}^{-1}$. Even if the source would be located at a distance of 8 kpc the inferred peak luminosity is a few times $10^{36} \text{ erg s}^{-1}$, still in the faint regime. However, such long distance is unlikely since the high Galactic latitude would place Swift J1357.2–0933 at 6 kpc above the Galactic plane.

The upper-limit on the luminosity inferred from the non-detections in the last two observations is $L_X \sim 2 \times 10^{31} \text{ erg s}^{-1}$. This could indicate that the nature of the accretor is a BH since they typically have quiescent luminosities in the range of $L_X \sim 10^{30} - 10^{31} \text{ erg s}^{-1}$ while the NS's usually have quiescent luminosities $L_X > 10^{32} \text{ erg s}^{-1}$ (but see Jonker et al. 2007).

The system was in the hard state at peak of the outburst and remained in this state during all the episode, which is usual at these low X-ray luminosities. From the first observation until the last one the spectral index of the power law increases from 1.5 to 2.2. As can be seen in Fig. 1, the X-ray luminosity and photon index are anti-correlated. The softening can also be checked in the HR curve demonstrating that it does not depend on assumed spectral model. It shows how the spectrum becomes softer as the luminosity decays (Fig. 1). Such softening behaviour was also present in the VFXT XTE J1719–291 (Armas Padilla et al. 2011), but for this source the spectra were considerably softer, with a photon index regime from $\Gamma=2.0$ to $\Gamma=2.7$. The reason for Swift J1357.2–0933 to have harder spectra than XTE J1719–291 could be a difference in the nature of their compact objects. Although it is not established,

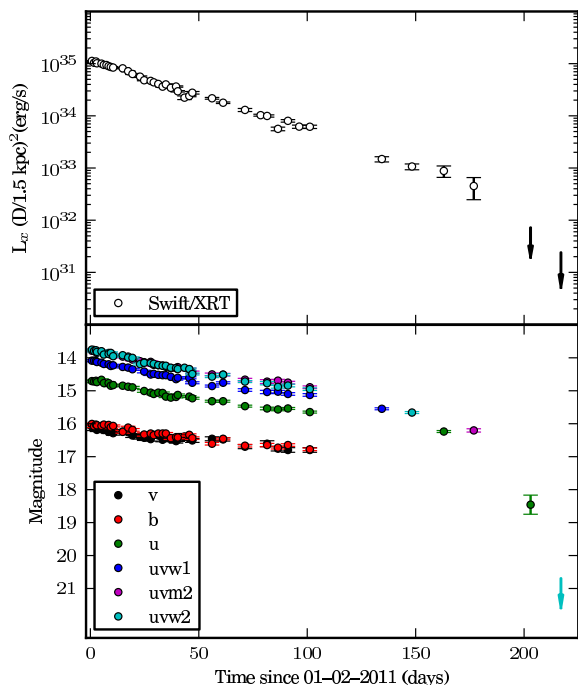


Figure 2. In the top panel the X-ray light curve in the 0.5–10 keV energy band for a distance of 1.5 kpc is shown while in the bottom panel the UV/optical light curves in the Vega system are plotted

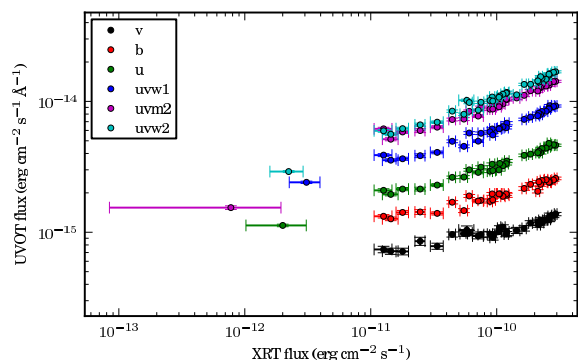


Figure 3. Correlation between the UV/optical density fluxes and the X-ray 2–10 keV flux.

the characteristics of XTE J1719–291 favour a NS accretor (Armas Padilla et al. 2011) whereas Swift J1357.2–0933 is a strong BH candidate system (Corral-Santana et al. 2012 in prep, private communication).

Several other BH sources have shown softening in their X-ray spectra at low luminosities. XTE J1650–500 softened in its 2001–2002 outburst. The photon index changed from $\Gamma=1.66$ to $\Gamma=1.93$ when the luminosity decayed to 2×10^{34} erg s $^{-1}$ (Tomsick et al. 2004). Also at this intermediate luminosities 4U 1543–47 evolved from a photon index of $\Gamma=1.64$ in its hard state to a photon index

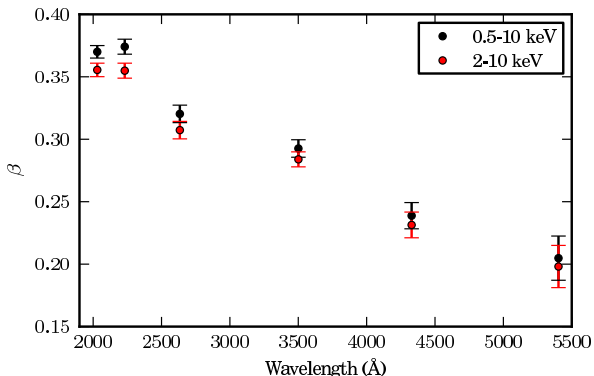


Figure 4. Correlation slopes (β) between the UVOT bands and the X-ray flux in the 0.5–10 keV and 2–10 keV energy bands.

of $\Gamma=2.22$ at lower L_X (Kalemci et al. 2005). By studying a sample of 7 BHs in their quiescence state, Corbel et al. (2006) arrived to the conclusion that all BHs are softer in quiescence than in the standard hard state. Using a study of 25 BHs, Dunn et al. (2010) presented data from which the same conclusion can be inferred: when data are available, the sources show softening towards quiescence. However, in the 2008 outburst decay of H 1743–322 to quiescence, Jonker et al. (2010) did not see any evidence of softening, although it cannot be ruled out that the cause is the inaccuracy in the photon index determination due to the high N_H .

4.1 X-ray and UV/optical simultaneous data: A non-irradiated accretion disc

The proximity and the low Galactic extinction towards Swift J1357.2–0933 have made it possible to obtain X-ray and UV/optical data simultaneously using XRT and UVOT instruments on board of *Swift*. Until today this had not been possible for any VFXT since, in addition to their low luminosity, the vast majority are located towards the Galactic centre, which makes it very difficult to detect the optical counterpart due to the high Galactic absorption.

The optical/UV and X-ray fluxes are strongly correlated during the outburst (Fig. 2). Russell et al. (2006) quantified the disc and jet contribution from the optical/infrared and X-ray (2–10 keV) correlation in the hard state. Based on the values tabulated in their work, our correlation in the v band is consistent with a BH accreting via a non irradiated viscous disc. Additionally, Frank et al. (2002) predict a dependency of the slopes β with the wavelength. For optical emission from a viscously heated steady-state disc, β increases at shorter wavelengths. This is consistent with our results, where β increases from 0.2 in the v band to 0.35 in the $uvw2$ one (see Table 2). Therefore, all the evidence favours UV/optical emission dominated by the viscously heated disc, with little or no X-ray irradiation detected.

ACKNOWLEDGMENTS

MAP acknowledges J. Corral-Santana and J. Casares for useful discussion on the nature of the source. RW was partly supported

by ERC starting grant awarded and partly by The European Community's Seventh Framework Programme (FP7/2007-2013) under grant agreement number ITN 215212 Black Hole Universe. ND is supported by NASA through Hubble Postdoctoral Fellowship grant number HST-HF-51287.01-A from the Space Telescope Science Institute (STScI). D.M.R is supported by a Marie Curie Intra European Fellowship within the 7th European Community Framework Programme under contract No. IEF 274805.

REFERENCES

- Armas Padilla M., Degenaar N., Patruno A., Russell D. M., Linares M., Maccarone T. J., Homan J., Wijnands R., 2011, *MNRAS*, 417, 659
- Chelovekov I. V., Grebenev S. A., 2007, *Astron. Lett.*, 33, 807
- Corbel S., Tomsick J. A., Kaaret P., 2006, *ApJ*, 636, 971
- Cornelisse R., Verbunt F., in't Zand J. J. M., Kuulkers E., Heise J., Remillard R. A., Cocchi M., Natalucci L., Bazzano A., Ubertini P., 2002, *A&A*, 392, 885
- Degenaar N., Wijnands R., 2009, *A&A*, 495, 547
- Del Santo M., Sidoli L., Mereghetti S., Bazzano A., Tarana A., Ubertini P., 2007, *A&A*, 468, L17
- Dunn R. J. H., Fender R. P., Körding E. G., Belloni T., Cabanac C., 2010, *MNRAS*, 403, 61
- Frank J., King A., Raine D. J., 2002, *Accretion Power in Astrophysics: Third Edition*
- Gehrels N., 1986, *ApJ*, 303, 336
- Jonker P. G., Miller-Jones J., Homan J., Gallo E., Rupen M., Tomsick J., Fender R. P., Kaaret P., Steeghs D. T. H., Torres M. A. P., Wijnands R., Markoff S., Lewin W. H. G., 2010, *MNRAS*, 401, 1255
- Jonker P. G., Steeghs D., Chakrabarty D., Juett A. M., 2007, *ApJ*, 665, L147
- Kalemci E., Tomsick J. A., Buxton M. M., Rothschild R. E., Pottschmidt K., Corbel S., Brocksopp C., Kaaret P., 2005, *ApJ*, 622, 508
- Krimm H. A., Barthelmy S. D., Baumgartner W., Cummings J., Fenimore E., Gehrels N., Markwardt C. B., Palmer D., Sakamoto T., Skinner G., Stamatikos M., Tueller J., Ukwatta T., 2011, *The Astronomer's Telegram*, 3138, 1
- Krimm H. A., Kennea J. A., Holland S. T., 2011, *The Astronomer's Telegram*, 3142, 1
- Pei Y. C., 1992, *ApJ*, 395, 130
- Rau A., Greiner J., Filgas R., 2011, *The Astronomer's Telegram*, 3140, 1
- Russell D. M., Fender R. P., Hynes R. I., Brocksopp C., Homan J., Jonker P. G., Buxton M. M., 2006, *MNRAS*, 371, 1334
- Schlegel D. J., Finkbeiner D. P., Davis M., 1998, *ApJ*, 500, 525
- Tomsick J. A., Kalemci E., Kaaret P., 2004, *ApJ*, 601, 439
- Wijnands R., in't Zand J. J. M., Rupen M., Maccarone T., Homan J., Cornelisse R., Fender R., Grindlay J., van der Klis M., Kuulkers E., Markwardt C. B., Miller-Jones J. C. A., Wang Q. D., 2006, *A&A*, 449, 1117